

Article

Computational Screening of Plant-Derived Natural Products against SARS-CoV-2 Variants

Waseem Ahmad Ansari ¹, Mohd Aamish Khan ¹, Fahmina Rizvi ¹, Kajim Ali ¹, Mohd Kamil Hussain ²,
Mohammad Saquib ³ and Mohammad Faheem Khan ^{1,4,*}

¹ Department of Biotechnology, Era University, Sarfarazganj, Hardoi Road, Lucknow 226003, India

² Department of Chemistry, Govt. Raza P.G. College, Rampur, M. J. P. Rohilkhand University, Bareilly 244901, India

³ Department of Chemistry, University of Allahabad, Prayagraj 211002, India

⁴ Department of Chemistry, Era University, Sarfarazganj, Hardoi Road, Lucknow 226003, India

* Correspondence: faheemkhan35@gmail.com

Abstract: The present study explores the efficacy of plant-derived natural products (PDNPs) against spike glycoproteins (S-glycoprotein) of SARS-CoV-2 variants using molecular docking, ADMET, molecular dynamics (MD) simulation and density-functional theory (DFT) analysis. In all, 100 PDNPs were screened against spike glycoprotein of SARS-CoV-2 variants, namely alpha (B.1.1.17), beta (B.1.351), delta (B.1.617), gamma (P.1) and omicron (B.1.1.529). Results showed that rutin, EGCG, hesperidin, withanolide G, rosmarinic acid, diosmetin, myricetin, epicatechin and quercetin were the top hit compounds against each of the SARS-CoV-2 variants. The most active compounds, rutin, hesperidin, EGCG and rosmarinic acid gave binding scores of -10.2 , -8.1 , -8.9 , -8.3 and -9.2 kcal/mol, against omicron, delta, alpha, beta and gamma variants, respectively. Further, the stability of docked complexes was confirmed by the analysis of molecular descriptors (RMSD, RMSF, SASA, Rg and H-bonds) in molecular dynamic simulation analysis. Moreover, the physicochemical properties and drug-likeness of the tested compounds showed that they have no toxicity or carcinogenicity and may be used as druggable targets. In addition, the DFT study revealed the higher activity of the tested compounds against the target proteins. This led us to conclude that rutin, hesperidin, EGCG and rosmarinic acid are good candidates to target the S-glycoproteins of SARS-CoV-2 variants. Further, in vivo and clinical studies needed to develop them as drug leads against existing or new SARS-CoV-2 variants are currently underway in our laboratory.

Keywords: SARS-CoV-2 variants; plant-derived natural products; molecular docking; molecular dynamic simulation; Density-Functional Theory



Citation: Ansari, W.A.; Khan, M.A.; Rizvi, F.; Ali, K.; Hussain, M.K.; Saquib, M.; Khan, M.F. Computational Screening of Plant-Derived Natural Products against SARS-CoV-2 Variants. *Future Pharmacol.* **2022**, *2*, 558–578. <https://doi.org/10.3390/futurepharmacol2040034>

Academic Editor: Fabrizio Schifano

Received: 21 October 2022

Accepted: 16 November 2022

Published: 19 November 2022

Publisher's Note: MDPI stays neutral with regard to jurisdictional claims in published maps and institutional affiliations.



Copyright: © 2022 by the authors. Licensee MDPI, Basel, Switzerland. This article is an open access article distributed under the terms and conditions of the Creative Commons Attribution (CC BY) license (<https://creativecommons.org/licenses/by/4.0/>).

1. Introduction

The recently discovered severe acute respiratory syndrome Coronavirus 2 (SARS-CoV-2), is a single-stranded RNA virus like the previously discovered severe acute respiratory syndrome Coronavirus (SARS-CoV), with 99.8% similarity in their gene sequences [1]. The SARS-CoV-2 genome has been found to be around 29.9 kB in size and comprises 27 distinct structural and non-structural proteins in addition to 14 open reading frames (ORFs). In the act of binding to host receptors, structural proteins such as spike glycoprotein (S), an envelope protein (E), nucleocapsid protein (N) and matrix protein (M) have been noted to play a significant role. Human angiotensin-converting enzyme 2 (ACE2) receptors are located on the cell surface, where they interact with spike proteins (S-protein), a trimeric protein, with tremendous affinity, to enable the SARS-CoV-2 genome to enter host cells [2,3]. The N-terminal S1 domain and the membrane-proximal S2 domain are the two subunits that make up the S-protein. Through the receptor-binding domain (RBD), the S1 domain identifies the ACE2 receptor on the cell surface; whereas, the S2 domain interferes with the

fusion of viral particles with the host cell membrane. Antibodies produced against SARS-CoV-2 are known to be neutralized by the RBD and other binding domains of S-protein [4]. As a result, it is possible to use the suppression of the S-glycoprotein and the human ACE2 receptor as they are prime targets for the development of COVID-19 remedies. It needs to be mentioned that the majority of the vaccines being administered to combat SARS-CoV-2 infection are typically based on S-glycoprotein sequences. Several anti-SARS-CoV-2 vaccine candidates only employ the RBD site as an antigen. SARS-CoV-2 is no different from those other viruses due to its ability to mutate. SARS-CoV-2 has more than 23,202 mutated variants which have been sequenced, and they spread and infect people more quickly, increasing the contagiousness of the virus. [5]. In particular, the United States (US), United Kingdom (UK), Brazil, South Africa and India have all seen a number of variants that exhibited increased transmissibility, immune evasiveness, more adaptable interaction of the spike protein to host receptors, as well as decreased vaccine efficacy because of mutations. Since there is no effective therapeutic agent currently available for the treatment of this viral infection, the entire world is still struggling to effectively combat and control SARS-CoV-2 and its variants.

Since ancient times, traditional medicine practitioners throughout the world have used medicinal plants in the treatment of various infections and disease conditions [6]. As demonstrated by numerous studies, traditional medicines in the form of crude extracts are rich sources of plant-derived natural products (PDNPs), such as polyphenols, flavonoids, terpenoids, alkaloids, steroids, tannins, lignans and fatty acids, which are also termed as secondary metabolites or phytochemicals. In the current drug-discovery scenario, PDNPs allow researchers to use them exclusively as drug-like lead molecules for the drug discovery and development processes [7]. For example, many studies revealed that polyphenols and flavonoids display promising antiviral properties including against HIV, influenza and dengue, as well as against COVID-19 [8]. Recently, we have also identified a few flavonoids namely quercetin, apigenin, myricetin, daidzein, epigallocatechin gallate (EGCG), genistein and luteolin, as well as other polyphenols such as ferulic acid, gingerol-6, piperine, resveratrol, etc. which inhibit SARS-CoV-2 by targeting its structural (spike protein) and non-structural proteins by using computational (molecular docking and molecular dynamic simulation) tools [9,10]. More recently, Agarwal et al. reported rutin as an effective inhibitor of the SARS-CoV-2 main protease (Mpro) with the help of a molecular docking study [11]. Furthermore, a group of NPs (e.g., withanolides), which are isolated from *Withania somnifera*, have shown COVID-19 inhibitory activity using *in silico* and *in vitro* methods [12]. Moreover, diosmetin, an important flavonoid of citrus lemon, significantly acts as predicting inhibitor of SARS-CoV-2 main protease as demonstrated by molecular docking, molecular dynamic simulations and quantum computational studies [13].

In this context, the aim of our study is to find out the possible drug leads of those PDNPs that are present in medicinal plants in good quantity against anti-SARS-CoV-2 variants by using computational tools. Based on the selection criteria, we have screened 100 PDNPs that are reported to have antiviral, anti-inflammatory and immunomodulatory properties in previous literature reports. A total of 100 PDNPs have been subjected to ADMET, drug-likeness and molecular docking studies to find out suitable inhibitory agents against SARS-CoV-2 variants namely alpha variant (B.1.1.17), beta variant (B.1.351), delta variant (B.1.617), gamma variant (P.1) and omicron (B.1.1.529), respectively. Among these, nine PDNPs viz. rutin, EGCG, hesperidin, withanolide G, rosmarinic acid, diosmetin, myricetin, epicatechin and quercetin exhibited better binding affinities to the S-glycoproteins of SARS-CoV-2 variants than the reference drug. The top hits ligands, hesperidin, EGCG, rosmarinic acid and rutin, were further evaluated through an MD simulation study to determine the stability of the ligand–protein interactions within the binding pockets of spike proteins of alpha, beta, gamma, delta and omicron variants, respectively. In addition, the DFT study revealed that hesperidin, EGCG, rosmarinic acid and rutin were found to show very good activity against each of the SARS-CoV-2 variants.

2. Materials and Methods

2.1. ADMET and Drug Likeness Study

Prediction of ADMET (absorption, distribution, metabolism, excretion and toxicity) is an important method in drug design and development processes. The ADMET properties were computed and calculated using SwissADME, internet server <http://www.swissadme.ch/index.php>, accessed on 21 May 2022. The drug-like properties including molecular weight (MW) (<500), lipophilicity (<4.15), hydrogen bond acceptor (HBA) (<10), hydrogen bond donor (HBD) (<5), topological polar surface area (TPSA) (<140 Å²), water-solubility (LogS), pharmacokinetics (gastrointestinal absorption, blood–brain barrier and permeability) and toxicity (mutagenic, tumorigenic, irritant and reproductive effect) have been performed by using Osiris Properties Explorer software [14].

2.2. Ligand Preparation

A library of 100 PDNPs from Indian medicinal plants with antiviral, anti-inflammatory and immunomodulatory properties was created for molecular docking investigations (Supplementary Tables S1–S5). The compounds were first screened from the PUBCHEM database (<https://pubchem.ncbi.nlm.nih.gov/>) to ensure their safety as spatial data file (SDF) and simplified molecular input line entry system (SMILES) format. The chemical structures of all the ligands were corrected for their properties, such as bond length and bond angles, before inserting missing hydrogen atoms. Prior to the molecular docking experiment, all ligands were entered from the workspace and optimised using the LigPrep module of Maestro version 12.6.144 Schrodinger 2020-4 LCC, New York USA programme with the force field OPLS3e which created possible states at the target pH. [15]. Following the preliminary results of molecular docking analysis, 9 PDNPs (three best compounds against each receptor) were chosen for further MD simulation, ADMET, and DFT studies and analysis.

2.3. Protein Preparation and Grid Generation

The structures of S-glycoproteins of all variants were available and thus obtained directly from the protein data bank (<https://www.rcsb.org/>) website. The 3D structures of all proteins, including alpha (PDB ID: 8DLI), beta (PDB ID: 7LYQ), delta (PDB ID: 7W92), gamma (PDB ID: 7SBT) and omicron (PDB ID: 7QO7) variants, were pre-processed and refined by using the protein preparation wizard in the Maestro version 12.6.144 Schrodinger 2020-4 LCC, New York USA suite. The selected receptor proteins were pre-processed by adding missing hydrogen atoms and converting selenomethionines to methionine. All hydrogen bonds were optimised using sample water orientation with PROPKA pH 7.0 while the receptor's energy was minimised using the default RMSD value 0.30 Å and OPLS3e force field methods. For generating the grid, we picked up the native ligands (NAG) that bound with residues in the active site of all the receptors including alpha, beta, gamma and omicron (Supplementary Figure S6). Because no native (crystallographic) ligand was found in the delta variant's 3D structure, we created the binding site using Goodford's grid algorithm via the sitemap tool and then used the default van der Waal 1.0 with 0.25 the partial charges cut-off scaling factors to create the grid map over the receptors [16,17].

2.4. Molecular Docking

Glide v8.8 (Schrodinger 2020-4 LCC, New York, NY, USA) software was used for the docking study to determine the binding affinities of ligands within the binding pockets of target proteins. The flexible molecular docking was performed by using HTVS (High Throughput Virtual Screening) precision. For the docking, the scaling factors were applied van der Waal radii 0.80 Å and a partial charge cut-off 0.15 Å was applied to the softening potential of ligands. Binding affinities were expressed as Glide scores for each ligand (PDNPs), obtained from project table. The final poses of complexes were visualised by the

pose viewer. Among them, the best poses were chosen based on the energy function that integrates the empirical and force field algorithm at the same time [18].

2.5. Molecular Dynamic Simulation

Following the molecular docking studies, the best-binding interacting complexes, hesperidin-alpha, EGCG-beta, rutin-delta, rosmarinic acid-gamma and rutin-omicron, were subjected to MD simulations experiments to examine their stability and confirm the molecular docking results using Desmond module of Schrodinger 2020-4 LCC, New York USA software. As previously indicated, the simulation was done with the OPLS-3e force field at 1000 trajectory frames of 100 ns time. The complex systems were then solvated by creating a transferable intermolecular potential 3P (TIP3P) water model with a box of 10.0 dimensions and periodic boundary condition (PBC) and neutralising the complexes with Na⁺/Cl⁻ ions. The final stage of the simulation was performed at a constant temperature 300 K along with isobaric isothermal ensemble (NPT equilibrium) by employing a Nose–Hoover chain thermostat at 300 K temperature 1 bar pressure after achieving equilibrium. The Particle–Mesh–Ewald summation (PME) approach was also used to determine the long-range electrostatic interactions between the atoms of ligand and protein. Finally, the interaction diagram was shown to analyse the trajectories of MD simulation trajectories using several parameters such as RMSD, RMSF, interacting Hydrogen bonds and radius of gyration (Rg) for the complexes [19,20].

2.6. DFT Calculation

The chemical characteristics of 4 PDNPs (rutin, hesperidin, EGCG, and rosmarinic acid), with the lowest binding energies in molecular docking and simulation processes against the control drug (nafamostat), are investigated using Density-Functional Theory (DFT). The DFT analysis (optimisation of shape and chemical characteristics) was conducted using Gauss View 6.0.16 and Gaussian 09W software and the B3LYP hybrid method at the 6-311G ground state. The optimum geometries of PDNPs were computed for HOMO and LUMO energies, as well as their gaps, and for showing the molecular electrostatic potential (MEP) map [21].

3. Results

3.1. Evaluation and Analysis of ADMET and Drug Likeness Properties

Lipinski's rule of five (Ro5), bioavailability score and drug score of all tested PDNPs utilised in this investigation were calculated using the SwissADME online server and Osiris Property Explorer, as shown in Tables 1 and 2. Among them, nine PDNPs (rutin, EGCG, hesperidin, withanolide G, rosmarinic acid, diosmetin, myricetin, epicatechin and quercetin) were chosen for further study due to higher bioavailability and drug score (bioavailability score > 0.50 and drug score > 0.30) to generate lead therapeutic agents against new SARS-CoV-2 variants (Figure 1). According to ADMET characteristics, epicatechin, quercetin, diosmetin and withanolide G have a high rate of human GI absorption, whereas EGCG, rutin, myricetin, rosmarinic acid and hesperidin have a low rate. The LogS number represents the drug's water solubility. The solubility of all evaluated PDNPs ranged from -2.22 to -4.32 [22].

Table 1. Results of ADME and drug-likeness properties of qualified PDNs.

Ligand	MW	HBA	HBD	TPSA	MLogP	LogS	GI	BBB	Ro5
Epicatechin	290.27	6	5	110.38	0.24	-2.22	High	No	Yes
EGCG	458.37	11	8	197.37	-0.44	-3.56	Low	No	No
Rutin	610.52	16	10	269.43	-3.89	-3.30	Low	No	No
Quercetin	302.24	7	5	131.36	-0.56	-3.16	High	No	Yes
Myricetin	318.24	8	6	151.59	-1.08	-3.01	Low	No	Yes

Table 1. Cont.

Ligand	MW	HBA	HBD	TPSA	MLogP	LogS	GI	BBB	Ro5
Diosmetin	300.26	6	3	100.13	0.22	−4.06	High	No	Yes
Rosmarinic acid	360.31	8	5	144.52	0.90	−3.44	Low	No	Yes
Hesperidin	610.56	15	8	234.29	−3.04	−3.28	Low	No	No
Withanolide G	454.60	5	2	83.83	3.48	−4.71	High	No	Yes
Nafamostat	347.37	4	4	140.57	2.96	−3.40	Low	No	Yes

MW = molecular weight, HBA = Hydrogen Bond Acceptor, HBD = Hydrogen Bond Donor, TPSA = Topological Polar Surface Area, MLogP = Lipophilicity, LogS = Water Solubility, GI = Gastrointestinal Absorption, BBB = Blood–Brain Barrier, Ro5 = Rule of Five.

Table 2. Results of toxicological properties of 10 PDNPs.

Ligand	Mutagenic	Tumorigenic	Irritant	Reproductive Effect
Epicatechin	No	No	No	No
EGCG	No	No	No	No
Rutin	No	No	No	No
Quercetin	Yes	Yes	No	No
Myricetin	Yes	No	No	No
Diosmetin	No	No	No	No
Rosmarinic acid	No	No	No	No
Hesperidin	No	No	No	No
Withanolide G	No	No	No	No
Nafamostat	No	No	No	No

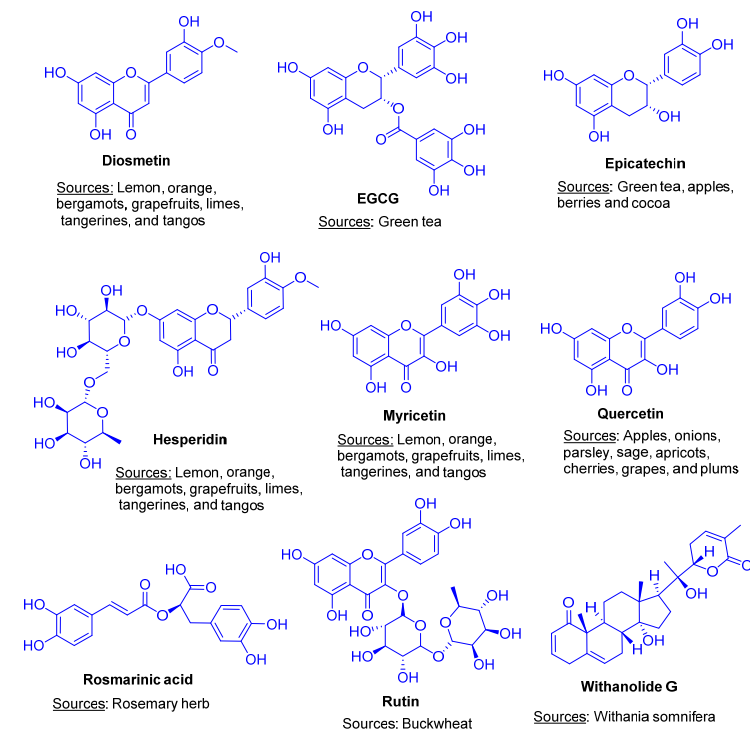


Figure 1. Chemical structures and sources of plant-derived natural products (PDNPs).

Furthermore, no PDNPs pass through the blood–brain barrier. EGCG, rutin and hesperidin had higher PSA values (>200.0), indicating that these compounds have stronger

druggable properties but other PDNPs (myricetin, quercetin, hesperidin, rosmarinic acid, withanolide-G, diosmetin, epicatechin) had lower PSA values (<100.0). As shown in Table 1, the molecular weight of EGCG, rutin, hesperidin, myricetin, quercetin, hesperidin, rosmarinic acid, withanolide-G, diosmetin and epicatechin are in the range of drug-likeness properties, except rutin and hesperidin [23]. In the toxicological study, quercetin and myricetin were predicted to be mutagenic and tumorigenic but other compounds showed no toxicity.

3.2. Evaluation and Analysis of Molecular Docking Analysis

The molecular docking approach has become a popular computer-aided virtual approach for screening drug targets in a short period of time while spending little energy and money on drug design and discovery. In order to search the therapeutic agents against the new variant of the SARS-CoV-2 virus, 100 PDNPs were initially screened based on their previously known antiviral properties [24]. They were subjected to molecular docking studies against said S-glycoproteins of SARS-CoV-2 variants. Using the lowest binding energy scale in comparison to the reference drug molecule “nafamostat”, the top three PDNPs for each variant were chosen for ADMET analysis. After that, the best PDNP for each variant was selected by combining docking and ADMET investigation for the molecular dynamic (MD) simulation study. Evaluation of the molecular docking study of 100 PDNPs yielded encouraging results against each of the SARS-CoV-2 variants. The reference drug nafamostat showed docking scores -5.324 , -5.665 , -5.340 , 4.260 and -5.325 Kcal/mole against omicron, delta, alpha, beta and gamma variants, respectively. Using these scores as filters, we chose the top 10 PDNPs which are rutin, hesperidin, ECG, EGCG, withanolide G, rosmarinic acid, diosmetin, myricetin, epicatechin and quercetin against all variants. Figure 2 depicts the 2D interactions of the best hits of PDNPs within protein receptor-binding sites in molecular docking, whereas molecular interactions are depicted in Table 3.

Table 3. Detail account of PDNPs, their molecular docking score against SARS-CoV-2 variants, and more active PDNPs shown in bold as compared to drug.

PubChem ID	Smiles	Compounds	Docking Score				
			Omicron	Delta	Alpha	Beta	Gamma
5280805	<chem>CC1C(C(C(O1)OCC2C(C(C(O2)OC3=C(OC4=CC(=CC(=C4C3=O)O)O)C5=CC(=C(C=C5)O)O)O)O)O)O</chem>	Rutin	-10.224	-8.160	-8.589	-8.095	-5.891
10621	<chem>CC1C(C(C(O1)OCC2C(C(C(O2)OC3=CC(=C4C(=O)CC(OC4=C3)C5=CC(=C(C=C5)OC)O)O)O)O)O)O</chem>	Hesperidin	-9.029	-7.873	-8.993	-7.559	-4.055
107905	<chem>C1C(C(OC2=CC(=CC(=C21)O)O)C3=CC(=C(C=C3)O)O)C(=O)C4=CC(=C(C=C4)O)O)O</chem>	ECG	-8.202	-7.454	-7.765	-7.429	-6.615
65064	<chem>C1C(C(OC2=CC(=CC(=C21)O)O)C3=CC(=C(C=C3)O)O)O)C(=O)C4=CC(=C(C=C4)O)O)O</chem>	EGCG	-7.700	-7.993	-7.851	-8.369	-7.532
21679023	<chem>CC1=C(C(=O)OC(C1)C(C)C2CC3(C2)C(C4C3CC=C5C4(C(=O)C=CC5)O)C)O)O)C</chem>	Withanolide G	-5.817	-6.159	-8.766	-6.590	-4.443
5281792	<chem>C1=CC(=C(C=C1CC(C(=O)O)OC(=O)C=CC2=CC(=C(C=C2)O)O)O)O</chem>	Rosmarinic acid	-6.739	-6.629	-8.761	-7.187	-9.235
5281612	<chem>COC1=C(C=C(C=C1)C2=CC(=O)C3=C(C=C(C=C3O2)O)O)O</chem>	Diosmetin	-7.659	-5.867	-6.173	-8.200	-6.439
5281672	<chem>C1=C(C=C(C=C1O)O)O)C2=C(C(=O)C3=C(C=C(C=C3O2)O)O)O)O</chem>	Myricetin	-6.877	-6.521	-6.916	-8.102	-5.968
72276	<chem>C1C(C(OC2=CC(=CC(=C21)O)O)C3=CC(=C(C=C3)O)O)O</chem>	Epicatechin	-7.596	-7.736	-7.799	-7.367	-8.896
5280343	<chem>C1=CC(=C(C=C1C2=C(C(=O)C3=C(C=C(C=C3O2)O)O)O)O)O</chem>	Quercetin	-6.092	-6.795	-6.825	-6.844	-8.021
4413	<chem>C1=CC(=CC=C1C(=O)OC2=CC3=C(C=C2)C=C(C=C3)C(=N)N)N=C(N)N</chem>	Nafamostat	-5.324	-5.665	-5.340	-4.260	-5.325

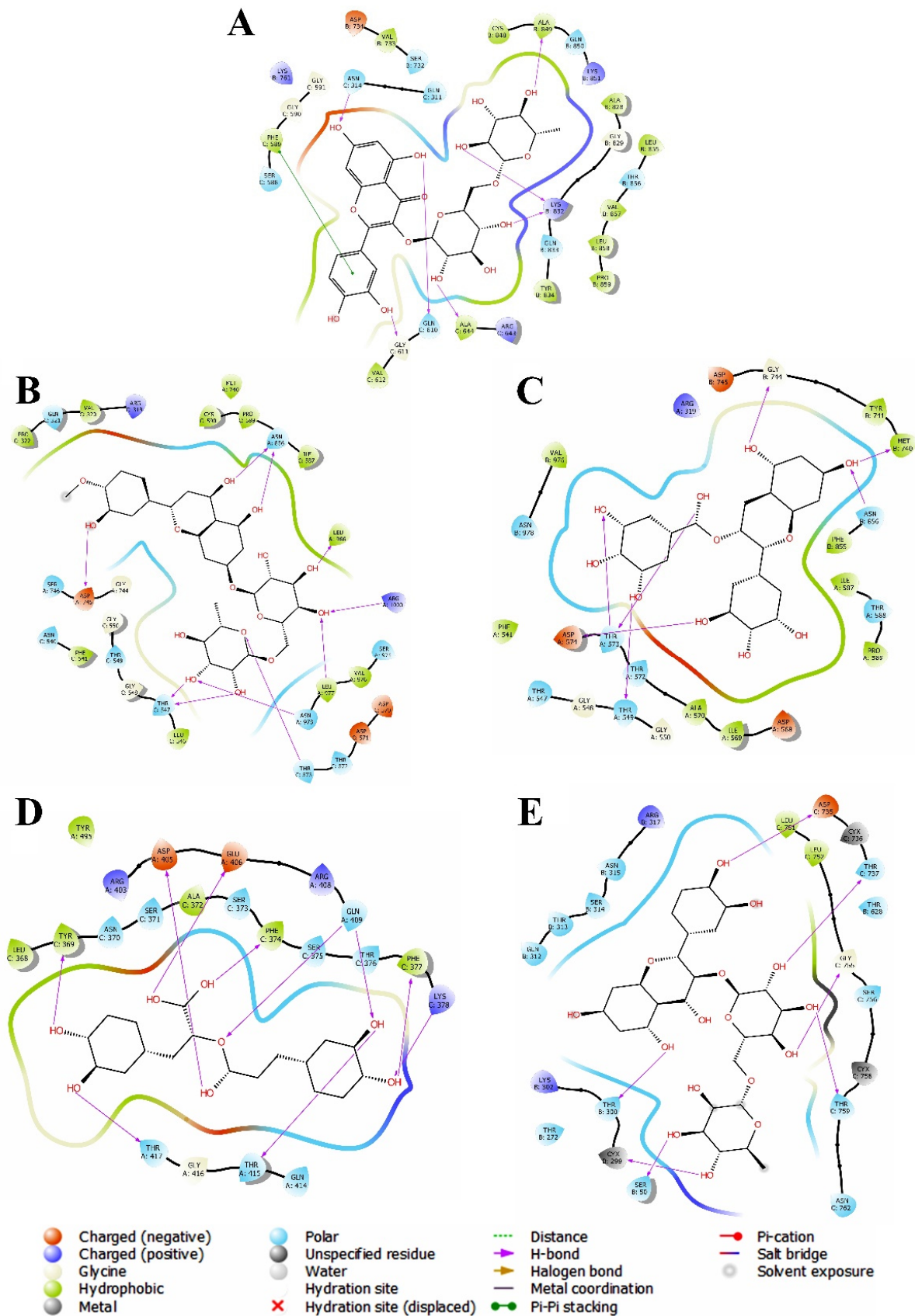


Figure 2. Two-dimensional view of molecular interactions in between (A) Rutin-S-protein of omicron variant, (B) Hesperidin and S-protein of alpha variant, (C) EGCG and S-protein of beta variant, (D) Rosmarinic acid and S-protein of gamma variant and (E) Rutin and S-protein of delta variant.

3.2.1. Molecular Docking against Omicron Variant

Among the top 10 PDNPs, rutin, hesperidin and ECG exhibited significant docking scores of -10.224 , -9.029 and -8.202 – 9.4 kcal/mol as compared to docking score of -5.324 kcal/mole for nafamostat against S-glycoprotein of omicron variant. By seeing molecular interactions, rutin binds with twenty-eight amino acids such as Asn314, Gln610, Gly611, Ala644, Lys832, Ala849, Gln311, Ser588, Gly590, Gly591, Val612, Arg643, Ser732, Val733, Asp734, Lys761, Ala828, Gly829, Gln833, Tyr834, Cys848, Gln850, Lys851, Leu855, Thr856, Val857, Leu858, Pro859 within binding pockets of the receptor protein. Hesperidin showed the interactions at Asn314, Gln610, Ile663, Ile309, Gln311, Phe589, Gly590, Gly591, Ser593, Leu608, Gly611, Arg643, Ala644, Pro662, Gly664, Lys730, Ser732, Val733, Asp734, Lys761, Thr765, Ala768, Val769, Lys832, Tyr834, Lys851, Gly854, Thr856, Val857, Leu858, Pro859, Leu861 amino acids. Moreover, ECG found to interact with Gly611, Gly835, Val548, Thr585, Pro586, Cys587, Ser588, Phe589, Val612, Asn613, Thr615, Glu616, Gln833, Tyr834, Asp836, Cys837, Lys851 amino acids [25].

3.2.2. Molecular Docking against Delta Variant

It was observed that three PDNPs, rutin, EGCG and hesperidin, have a more negative docking score than the control drug nafamostat drug (Table 3). With a docking score of -8.160 , rutin formed nine chemical contacts with Ser50, Cys299, Thr300, Asp735, Thr737, Gly755, Thr759, Leu51 and Leu52 amino acid residues (Figure 2). EGCG docked with a docking score of -7.993 , when interacting with the amino acid residues Thr272, Thr300, Thr313, Asn315, Thr737, Thr759, Asn762, Leu751 and Leu752. Furthermore, with a docking score of -7.873 , hesperidin was found to bind at active sites with the amino acid residues Gln52, Ser314, Gly755, Thr759, Leu301, Leu752 and Phe757. According to our results, rutin is the most effective against the delta variant followed by EGCG and hesperidin, respectively [26].

3.2.3. Molecular Docking against Alpha Variant

In the case of the alpha variant, hesperidin, withanolide G and rosmarinic acid outperformed the nafamostat in terms of docking score against S-glycoproteins. Hesperidin binds with the amino acids Thr547, Thr573, Asp745, Asn856, Leu977, Asn978, Arg1000, Val320, Pro322, Phe541, Leu546, Ile587, Pro589, Cys590, Met740, Val976 and Leu977 to establish seventeen chemical interactions. Likewise, withanolide G showed thirteen molecular interactions with the amino acid residues Thr549, Asn856, Asn978, Pro322, Val320, Phe541, Leu546, Ile587, Pro589, Cys590, Phe592, Met740 and Val976 whereas the functional moieties of rosmarinic acid were found to interact with Thr547, Thr549, Thr573, Tyr741, Asn856, Asn57. Finally, hesperidin was found to be more effective against the alpha variant followed by withanolide G and rosmarinic acid [27].

3.2.4. Molecular Docking against Beta Variant

When compared to nafamostat, EGCG, diosmetin and myricetin had significantly higher binding affinities against S-glycoprotein of the beta variant. The fourteen interactions between EGCG and the amino acids Thr549, Thr573, Asp574, Met740, Gly744, Asn856, Phe541, Ile569, Ala570, Ile587, Pro589, Tyr741, Phe855 and Val976 resulted in a docking score of -8.369 . While myricetin docked with a significant docking score (-8.102) via interactions with Thr549, Thr573, Met740, Gly744, Phe541, Ile587, Pro589, Tyr741, Cys743, Leu966, Val976 and Leu977 amino acid residues, diosmetin docked with a docking score of -8.200 , via interaction with these same amino acid residues: Ile587, Met740 (Figure 2). Finally, the binding energy is shown to be in the following order: EGCG > diosmetin > myricetin [28].

3.2.5. Molecular Docking against Gamma Variant

The PDNPs rosmarinic acid, epicatechin and quercetin were found to have docking scores -9.235 , -8.248 and -7.925 kcal/mole, respectively, compared to nafamostat's

docking scores -5.325 kcal/mole against S-glycoprotein of gamma variant. Rosmarinic acid binds to the following amino acid residues: Thr369, Lys378, Asp405, Glu406, Gln409, Thr415, Phe374, Phe377, Thr417, Leu368, Ala372 and Tyr495. Furthermore, epicatechin and quercetin both interacted with the following amino acid residues: Tyr369, Ser371, Phe374, Phe377, Lys378, Arg408, Gln409, Thr417, Leu368 and Ala372, respectively. Finally, the binding energy is shown to be in the following order: rosmarinic acid > epicatechin > quercetin [29].

3.3. Evaluation and Analysis of Stability in Complexes through MD Simulation

MD simulation is a computer-calculated approach for obtaining dynamic data at atomic spatial resolution during ligand-protein complex formation. The MD simulation study was performed for 100 ns to analyse the structural characteristics and stabilities of best-docked complexes such as rutin-omicron, rutin-delta, hesperidin-alpha, EGCG-beta, rosmarinic acid-gamma, obtained by molecular docking studies [30].

3.3.1. RMSD and RMSF Analysis

Firstly, RMSD analysis was carried out where the rutin-omicron complex exhibited a transitory movement up to 5 ns with an RMSD value of 14.75 Å, followed by achieving equilibrium inside the active regions of the protein and finally, rutin sustained the stability up to end of the simulation. The complex of rutin-delta showed conformational changes from beginning up to 55 ns at RMSD range ranging from 1.0 to 3.5 Å, beyond 60 ns RMSD, stability increases and remains constant up to 90 ns of the entire simulation. In the case of the hesperidin-alpha complex, only slight variations in stability were seen at the start of the simulation. The hesperidin demonstrated consistent RMSD between 20 to 90 ns with an RMSD range of 2.4 to 4.0 Å.

The RMSD plots of the EGCG-beta complex as well as and rosmarinic acid-gamma complex show a considerable number of conformational changes but no appreciable stability. Figures 3 and 4 showed the RMSD and RMSF values. The RMSD values of the C α atoms as shown in Table 4 were determined to be 2.48 – 34.46 Å, 2.192 – 4.272 Å, 2.213 – 5.801 Å, 2.758 – 79.25 Å and 2.008 – 7.086 Å for the S-glycoproteins in the complexes of omicron, delta, gamma, beta and alpha variants, respectively. Furthermore, RMSD data were supported by root mean square fluctuations (RMSF) plots of the local changes in residues per atom in obtained complexes. The RMSF plots were created to better comprehend the flexibility of each residue in protein complexes. The fluctuation in each residue is estimated using the RMSF values of protein C α atoms which were, later on, found to be 1.91 – 17.43 Å (rutin-omicron), 0.051 – 9.242 Å (rutin-delta), 0.616 – 9.723 Å (hesperidin-gamma), 11.057 – 34.333 Å (EGCG-beta), 0.254 – 9.756 Å (rosmarinic acid-alpha), respectively [31]. Thus, RMSF confirms the conformational changes in protein structures after binding with these compounds.

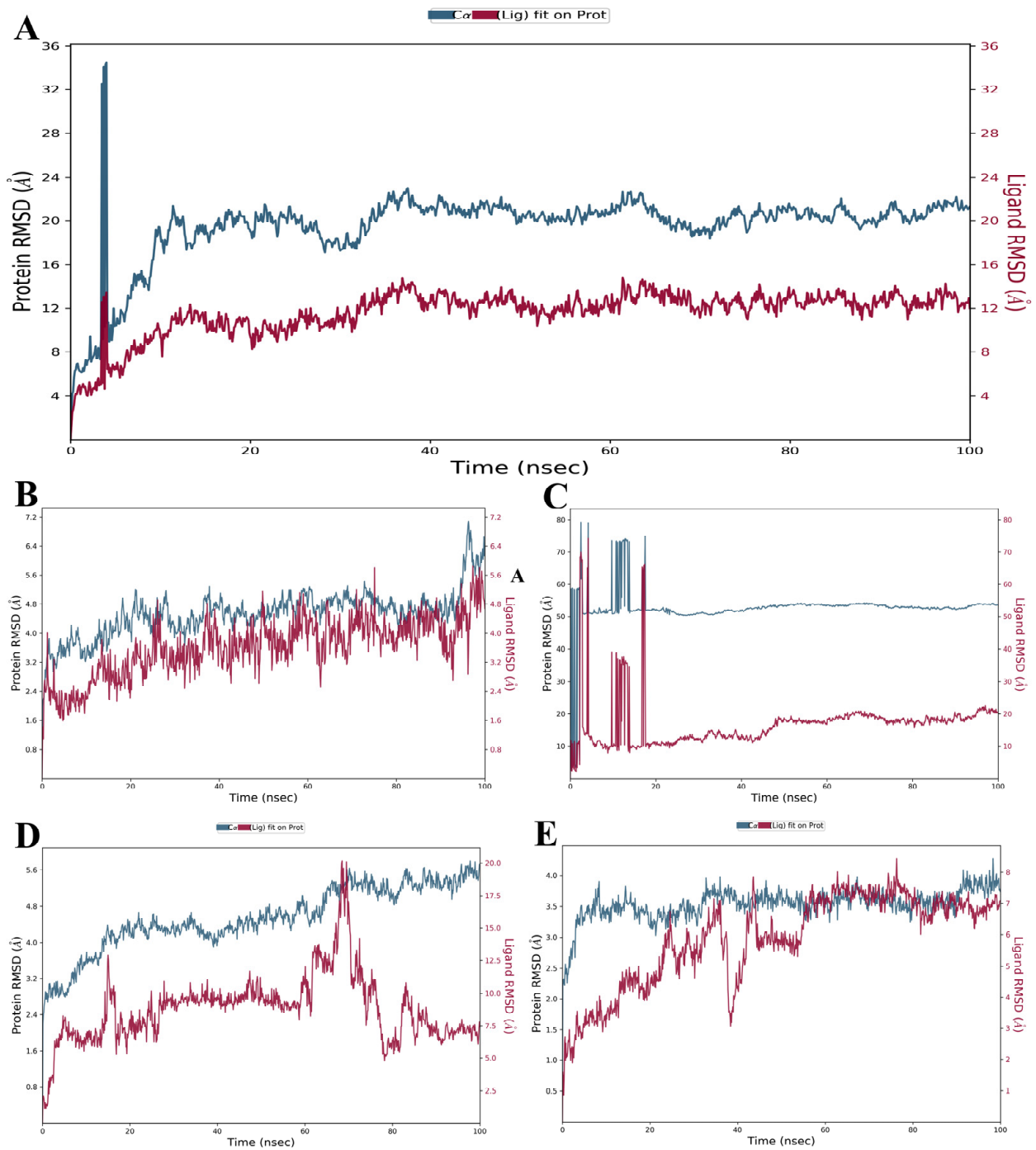


Figure 3. RMSD analysis of (A) Rutin-omicron complex, (B) Hesperidin-alpha complex, (C) EGCG-beta complex, (D) Rosmarinic acid-gamma complex and (E) Rutin-delta variant complex for 100 ns MD simulation.

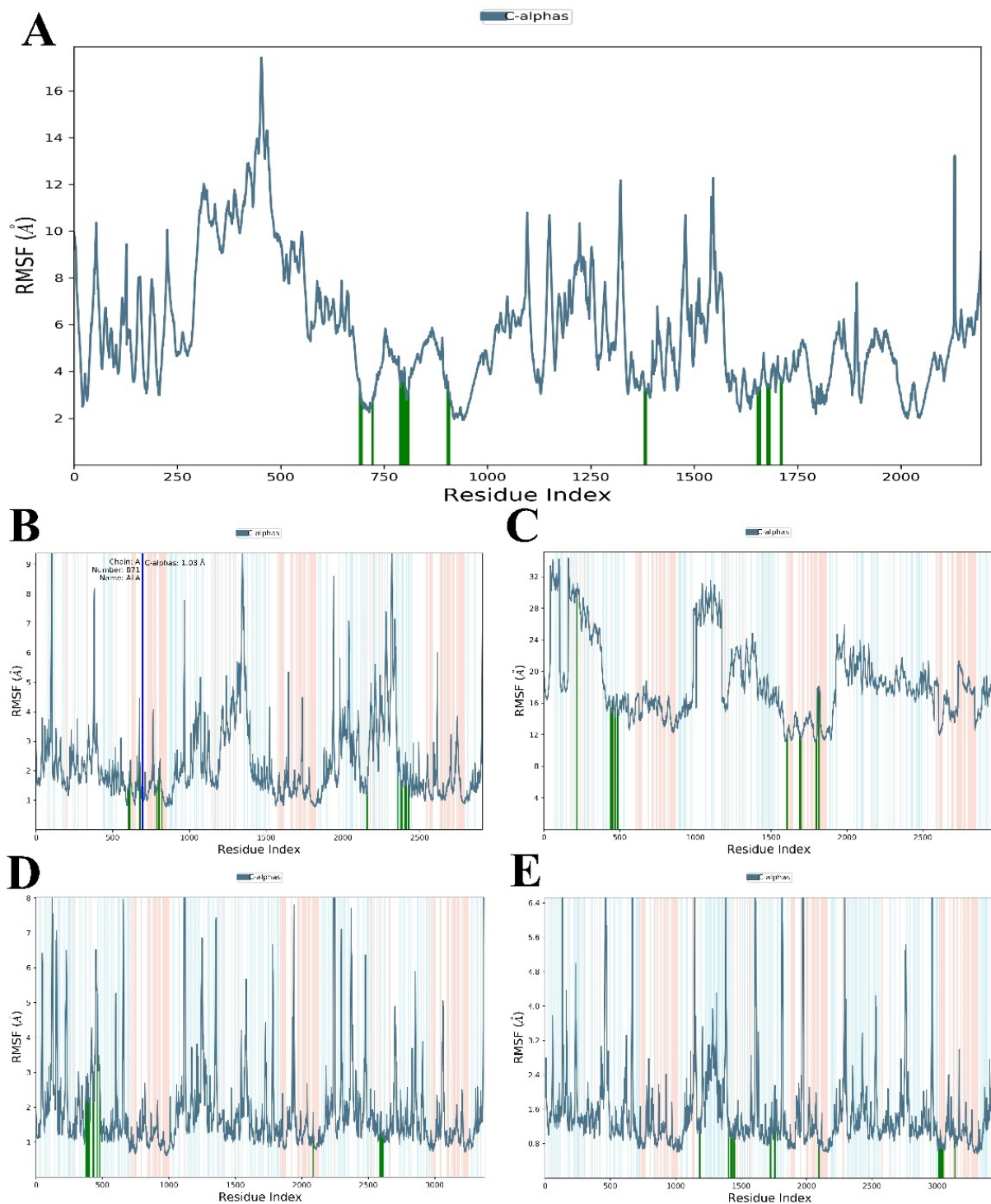


Figure 4. RMSF analysis of (A) Rutin-omicron complex, (B) Hesperidin-alpha complex, (C) EGCG-beta complex, (D) Rosmarinic acid-gamma complex and (E) Rutin-delta complex for 100 ns MD simulation. The graphs are displaying protein residue fluctuations (light blue curves), residues in interaction with the ligand shown by green vertical lines; salmon and cyan rectangles display alpha-helical and beta-stranded domains, respectively. Only active residues in the S-glycoprotein of all the variants are simulated.

Table 4. Details of properties of complexes obtained during MD simulation.

Properties	Omicron Variant	Delta Variant	Gamma Variant	Beta Variant	Alpha Variant
RMSD value (Å) (Protein)	2.48–34.46	2.19–4.27	2.21–5.80	2.75–79.25	2.00–7.08
RMSD value (Å) (Ligand)	1.29–14.75	0.85–8.42	1.09–20.16	2.16–74.14	1.01–5.84
RMSF value (Å) (Protein)	1.91–17.43	0.05–9.24	0.61–9.72	11.05–34.33	0.254–9.75
Rg (Å)	4.68–5.34	4.46–5.30	3.68–5.12	4.18–4.60	4.76–5.90
SASA (Å ²)	20.85–152.19	78.64–246.68	10.77–605.76	306.64–522.23	59.43–365.01
PSA (Å ²)	434.30–479.31	408.97–476.18	235.79–321.38	346.76–409.92	356.01–426.20

3.3.2. Radius of Gyration (Rg) Analysis

The radius of gyration (Rg) helps to determine the compactness of the protein–ligand complexes [32,33]. To examine the compactness and structural changes of formed complexes, the Rg value was calculated and analysed, with a larger value indicating less compactness of folded protein and a lower value indicating greater compactness of folded protein. Table 4 presented the Rg values while Figure 5 shows the Rg plots of formed complexes. The average Rg for the rutin-omicron complex was 4.68–5.34 Å while the rutin-delta complex exhibited an average Rg value of 4.466–5.307. Over 100 ns simulation, the average Rg value in the rosmarinic acid-gamma complex was 3.687–5.124; whereas, it was observed as 4.763–5.908 in the hesperidin-alpha complex and 4.187–4.609 in the EGCG-beta complex. The complexes stayed intact throughout the 100 ns simulation frame of time.

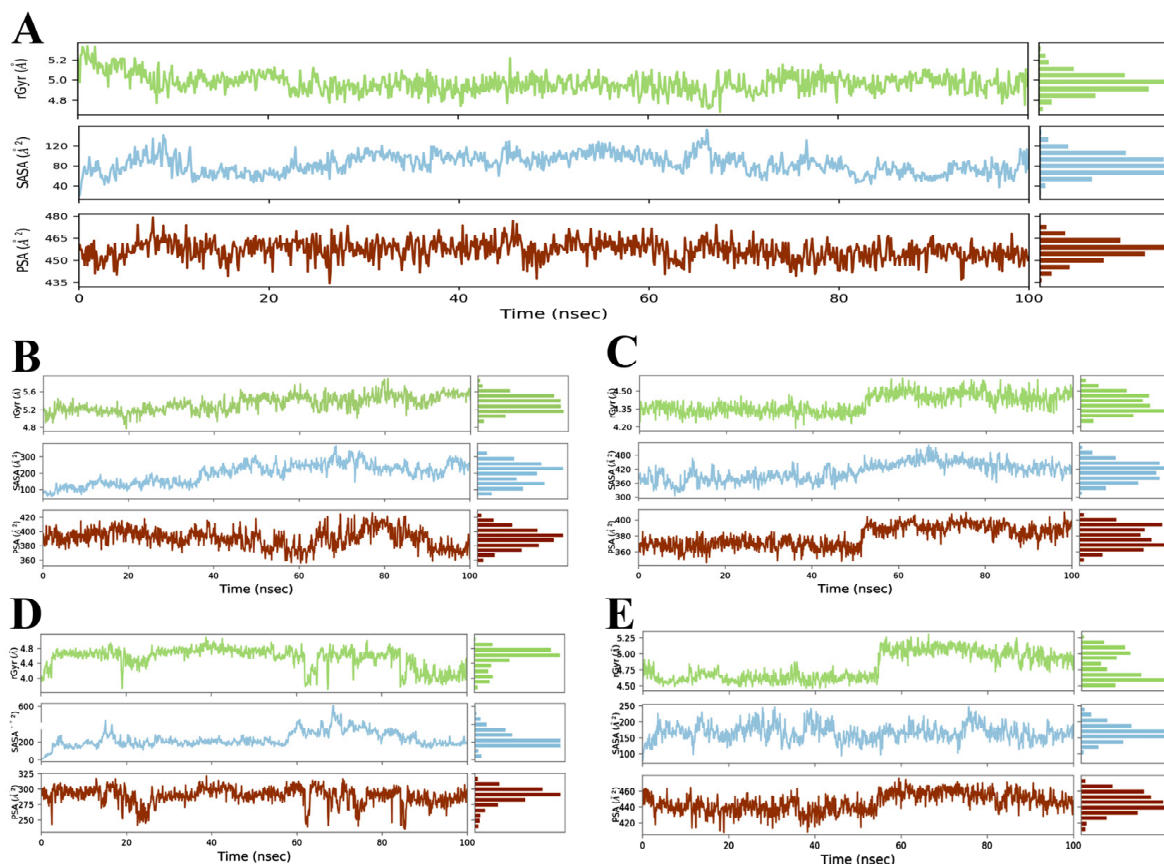


Figure 5. Ligand properties during the complex formation at 100 ns simulation trajectory: (A) Rutin-omicron complex, (B) Hesperidin-alpha complex, (C) EGCG-beta complex, (D) Rosmarinic acid-gamma complex and (E) Rutin-delta complex.

3.3.3. Solvent Accessible Surface Area (SASA) Analysis

In addition, we used the solvent-accessible surface area (SASA) analysis to anticipate the interactions between solvent and complexes during the simulation [34]. The SASA values can be computed by dissolving protein cavities, and observing residue rearrangement during protein–ligand interactions. Table 4 and Figure 5 show the average SASA values 20.85–152.19 for the omicron variant; 78.643–246.681 for rutin-delta; 10.778–605.765 for hesperidin-gamma; 306.646–522.238 for EGCG-beta; and 59.436–365.014 for rosmarinic-alpha complexes throughout a 100 ns simulation period.

3.3.4. Polar Surface Area (PSA) Analysis

Polar surface area (PSA) is the sum of the surface area covered by polar moieties such as oxygen and nitrogen atoms. PSA is used to calculate the values of molecular descriptors for studying intestinal absorption and blood–brain barrier (BBB) penetration properties. The PSA values of less than 200 Å² (for intestinal absorption) and less than 60 Å² (for blood–brain barrier penetration) have been identified as good predictors of drug absorption [35]. The computed PSA values for the compounds within the complexes were 434.30–479.31 (omicron variant), 408.977–476.184 (delta variant), 235.797–321.389 (gamma variant), 346.765–409.927 (beta variant) and 356.019–426.209 (alpha variant), respectively, as shown in Table 4. However, according to value analysis, they do not have adequate intestinal and blood–brain barrier penetration because their PSA values are greater than 200 Å² and 60 Å², respectively.

3.4. Evaluation and Analysis of Density-Function Theory (DFT) Method

The optimised structures of the top 4 hits (rutin, hesperidin, EGCG, rosmarinic acid) and their geometrical parameters are displayed in Figures 6 and 7 as well as Table 5, by using DFT/B3LYP hybrid approach on the 6-311G basis set. The chemical reactivity of the top four hits was determined using frontier molecular orbital (FMO) and molecular electrostatic potential (MEP) plots. The FMO theory is utilised to investigate the highest occupied molecular orbital (HOMO) and lowest unoccupied molecular orbital (LUMO) via electron donation and acceptance Figures 6 and 7. The HOMO energies were predicted to be –5.74 eV (rutin), –5.57 eV (hesperidin), –5.90 eV (EGCG), –5.94 eV (rosmarinic acid) and –5.78 eV (nafamostat), while the LUMO energies were determined to be –1.75 eV (rutin), –1.84 eV (hesperidin) and –1.68 eV (EGCG). As a result, the energy gap (Egap) for the HOMO-LUMO investigation was determined to be 3.99 eV (rutin), 3.73 eV (hesperidin), 4.22 eV (EGCG) and 3.78 eV (rosmarinic acid), as shown in Table 5 [36]. They have a lower energy gap than nafamostat with the value of 4.25 eV, indicating that they are reactive to the protein receptors. The MEP surface exhibits the compound's reactive sites based on colour indications ranging from dark red (nucleophile) to dark blue (electrophile) regions. In our computed study, rutin, hesperidin, EGCG and rosmarinic demonstrated nucleophilicity with the value of -8.230×10^{-2} au, -8.796×10^{-2} au, -8.080×10^{-2} au and -8.538×10^{-2} au, whereas electrophilicity was estimated with values of 8.230×10^{-2} au, 8.796×10^{-2} au, 8.080×10^{-2} au and 8.538×10^{-2} au. On the other hand, for nafamostat, the nucleophilicity and electrophilicity values were -7.178×10^{-2} au and 7.178×10^{-2} , respectively [37]. According to our findings, rutin, hesperidin, EGCG and rosmarinic acid are the top hits for identifying inter- or intramolecular interaction sites in S-glycoproteins of SARS-CoV-2 variants.

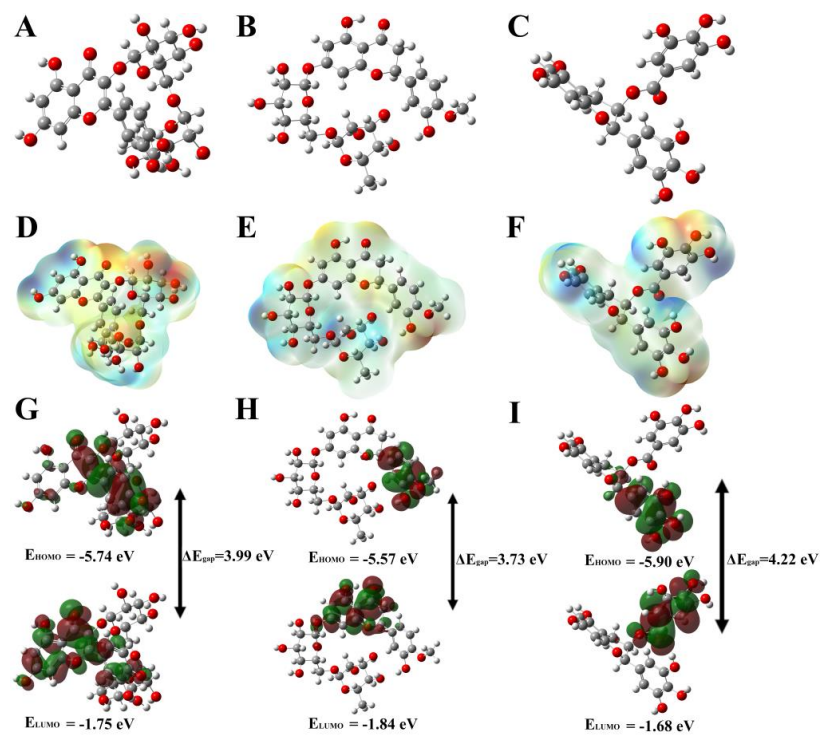


Figure 6. Geometrically optimised structures of rutin (A), hesperidin (B) and EGCG (C); Molecular electrostatic potential surfaces of rutin (D), hesperidin (E) and EGCG (F), and HOMO-LUMO energy gaps of rutin (G), hesperidin (H) and EGCG (I).

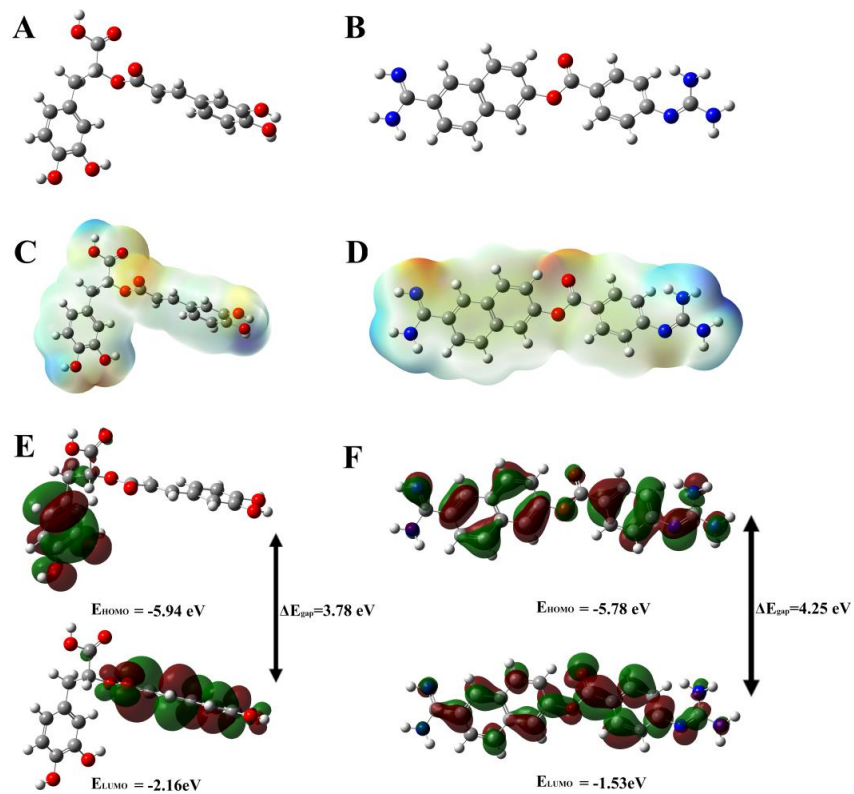


Figure 7. Optimised structures of rosmarinic acid (A) and nafamostat (B); Molecular electrostatic potential surfaces of rosmarinic acid (C) and nafamostat (D); HOMO-LUMO energy gaps of rosmarinic acid (E) and nafamostat (F).

Table 5. DFT calculations of best hits of PDNPs.

Compounds	HOMO	LUMO	* ΔE_{gap}
Rutin	−5.74	−1.75	3.99
Hesperidin	−5.57	−1.84	3.73
EGCG	−5.90	−1.68	4.22
Rosmarinic acid	−5.94	−2.16	3.78
Nafamostat	−5.78	−1.53	4.25

* All the values are in eV.

4. Discussion

Mutations in the S-glycoprotein of coronavirus, which interact with the transmembrane protein (ACE2) of human cell receptors have resulted in the emergence of several variations of SARS-CoV-2. The interactions between S-glycoprotein and ACE2 are critical for virus entry into host cells, thereafter facilitating the replication of the viral genome [38]. It is now evident that in the continuous mutations in S-glycoproteins, SARS-CoV-2 variants may also act as resistance against drug action and vaccine-induced acquired immunity. Inhibition of S-glycoprotein and ACE2 may, thus, serve as therapeutic targets for the discovery and development of anti-COVID-19 inhibitors [39]. Recently it has been seen that medicinal plants and their chemical constituents may act as safe and alternative agents to manage the COVID-19 disease. Therefore, in order to continue our research into PDNPs as therapeutic agents, we chose 100 PDNPs that have already been established to have antiviral properties, and then, assessed them against the S-glycoproteins of SARS-CoV-2 variants. To compare our findings, we used nafamostat (S-glycoprotein inhibitor) as a reference drug. Prior to performing the thorough analysis, we conducted a preliminary docking study and discovered 9 PDNPs (diosmetin, EGCG, epicatechin, hesperidin, myricetin, quercetin, rosmarinic acid, rutin and withanolide-G) with more negative binding energy than nafamostat. Later on, nine PDNPs were subjected to detailed MD simulation and ADMET by using Glide v8.8 (Schrodinger, LLC, New York, NY, USA) software to assess how and in what way, these PDNPs inhibited the S-glycoproteins of said variants. The usage of herbs and medicinal plants containing a significant amount of PDNPs has a long history in the prevention of respiratory diseases including the common cold, flu, cough, etc., which are caused by both bacteria and viruses [40]. A number of PDNPs obtained from gingers, turmeric, giloy, black pepper, tulsi, ashwagandha, green tea, etc., have shown beneficial effects against SARS-CoV-2 infection as per in silico studies [41]. Polyphenols, particularly flavonoids, have been extensively studied for their antiviral activity against hepatitis viruses, dengue viruses, Epstein–Barr viruses, herpes viruses, influenza viruses, HIV, rotaviruses and coronaviruses. Although the precise mechanism of action is uncertain, they reduced viral infection in host cells by preventing virus entry or decreasing virus multiplication. Several studies have shown that tea polyphenols have antiviral properties by inhibiting DNA viruses such as herpesviruses, papillomaviruses, poxviruses and HIV-1. In a dose-dependent way, resveratrol, ferulic acid and gallic acid greatly suppressed the expression of Epstein–Barr Virus lytic genes. Furthermore, resveratrol has been shown to inhibit respiratory viruses such as rhinoviruses and syncytial viruses, as well as Varicella-zoster, a virus that causes fever and a vesicular rash. Furthermore, Chojnacka et al. summarised a study based on the analysis of several studies and concluded that ellagic acid, myricetin, kaempferol and quercetin exhibited anti-influenza activity, whereas cyanidin-3 rutinoside, cyanidin-3-glucoside, rutin and gallic acid were found to show inhibitory activity against the H1N1 influenza virus via an inhibiting viral attachment or by influencing viral entrance inhibition into host cells [42,43].

Additionally, because computational approaches are straightforward, quick and economical, they are a useful tool for the discovery and development of drugs based on bioactive natural products. To provide 2D and 3D molecular profiles of natural products, they construct pharmacophore models, molecular interaction fields, docking and simula-

tions of complexes. Because experimental procedures are time-consuming, expensive and replete with errors when a suitable protein target is lacking, computational tools can be used to enhance the pharmacological efficacy and safety of natural products as well as their further development. Polyphenols are a diverse class of natural compounds that serve a variety of biological functions. Their anti-inflammatory and antioxidant effects are well established. They have been investigated for antiviral properties, including the recently found SARS-CoV-2, which has wreaked havoc due to its high infectivity and mortality rate. Many research organisations found different therapeutic compounds from medicinal plants in a relatively short period of time, attributable to computational strategies in research. The majority of research has concentrated on polyphenols because of their antiviral characteristics, which have been widely documented in prior works. Furthermore, substantial research has been conducted in the last two years on natural products that demonstrate high anti-SARS-CoV-2 activity, but no report on natural products as inhibitory agents of various SARS-CoV-2 variants is known. As a result of these findings, we conducted a thorough cross-analysis of previously published pharmacological and computational research including the polyphenols identified in our study as anti-S-glycoprotein of SARS-CoV-2 variants [44–46].

In some studies, EGCG was reported to exhibit anti-COVID-19 properties by fighting SARS-CoV as well as its mutant version B.1.1.7, preventing the viral replication and viral entry into the host cells; whereas, epicatechin had no inhibitory impact on SARS-CoV-2 [47]. As per our findings, EGCG firmly attached to the binding pockets of S-glycoproteins of delta and beta variants with significant docking scores whereas epicatechin exhibited greater binding affinity to the S-glycoprotein of the gamma variant than the nafamostat. Thus, we may conclude that EGCG and epicatechin can effectively kill SARS-CoV-2 and its variant. Yusuf A. Haggag et al. demonstrated the potential use of hesperidin in prophylaxis and treatment of COVID-19 and then hypothesized that hesperidin would reduce the entry of SARS-CoV-2 by blocking the ACE2 human receptor [48]. Moreover, hesperidin has also been found to inhibit SARS-CoV-2 infection by reducing the interaction of S-glycoprotein and human ACE2 receptor as well as TMPRSS2 expression in VeroE6 cells using lentivirus-based pseudo-particles of SARS-CoV-2 and its new variants [49]. When we computed the hesperidin, we discovered that it had substantial binding affinity against S-glycoproteins of both delta and alpha variants. The binding energies of hesperidin against both the said variants were more significant than the binding energy of nafamostat and therefore, it may prevent the entry of delta and alpha variants into the human body.

In our study, quercetin and its glycoside rutin demonstrate strong binding efficacy within the binding grooves of S-glycoproteins of gamma and delta variants, displaying effective docking scores when compared to nafamostat. Our results were very similar to the experimental as well as virtual studies, which have been done earlier, where both the compounds were found to cleave the 3CLpro at catalytic dyad (His41/Cys145) of S-glycoprotein and thus, quercetin and rutin may inhibit SARS-CoV-2 and its variants [50]. In the case of diosmetin and myricetin, both are flavonoids, have promising computed results against COVID-19 infection. Jishan Khan et al. have reported the protective effect of diosmetin against COVID-19 disease by inhibiting Mpro of SARS-CoV-2 using a virtual study [13]. In a study, Xiao et al. show the inhibitory activity of myricetin against SARS-CoV-2 Mpro with $IC_{50} 3.684 \pm 0.076 \mu M$ in the enzyme assay using the fluorescence-resonance energy-transfer method. Myricetin also suppressed pulmonary inflammation by inhibiting the overexpression of inflammatory cytokines such as IL-6, IL-1 α , TNF- α and IFN- γ which are expressed during COVID-19 infection as shown in a different study [51]. In order to our findings, it is predicted that diosmetin and myricetin may act as excellent inhibitory agents of S-glycoprotein of beta variant. Overall, these results indicate that both diosmetin and myricetin could inhibit S-glycoproteins that restrict the entry of beta variants through the human ACE2 receptor.

Based on previous reports, withanolides, steroidal lactones of Indian Ashwagandha, have been predicted as lead PDNPs based on drug-likeness or drug-ability properties,

molecular docking and MD simulation studies to combat COVID-19 infection via inhibiting Mpro, 3CLpro, and spike protein of SARS-CoV-2 as well as to strengthen the immune system in those patients [52,53]. To check its efficacy against different variants, we have predicted that withanolide G shows strong binding affinity with a promising docking score against the S-glycoprotein of the alpha variant and thus inhibited effectively the attachment of the virus with the human ACE2 receptor. Elebeedy et al. reported the encouraging outcomes from the inhibitory potential of rosmarinic acid for S-glycoprotein of SARS-CoV-2 using molecular docking study as well as in vitro assay with the help of plaque reduction and MTT assay on Vero E6 cells. In this study, rosmarinic acid exhibited a significant IC_{50} value equal to 15.37 ng/ μ L [54]. Our results predict that rosmarinic acid acts as a strong inhibitory agent against alpha and gamma variants because it strongly binds to the S-glycoproteins of both variants, possessing -8.761 and -9.235 binding energies, respectively.

By elaborating ADMET parameters, lipophilicity and solubility play a key role in favorable drug development by evaluating the absorption and skin permeation effects [55]. In our findings, these PDNPs have good absorption (lower than -5.0) values, showing drug-likeness behaviour. These compounds have good penetration power and reach the target receptor molecule through any barrier because of good distribution values. The topological polar surface area is related to the total polar surface covered by all the atoms in a compound. The topological polar surface area of screened compounds lied in between 83.83 \AA^2 to 269.43 \AA^2 values, which is good for drug design. As per Ro5, it is believed that a compound should have certain pharmacological properties that would make it fit or/not fit as an orally active therapeutic agent for human consumption (e.g., a molecule with a molecular mass <500 Da, <5 HBD, <10 HBA and an octanol-water partition coefficient <5) [56]. Among the tested PDNPs, six compounds namely epicatechin, EGCG, quercetin, myricetin, rosmarinic acid, diosmetin and withanolide G qualified the Lipinski's Ro5 except for EGCG, rutin and hesperidin as their value were outpaced the standard value of 5. Hence, they might be good chemical agents for drug design and development against COVID-19. Considering all these parameters, all nine compounds (epicatechin, EGCG, rutin, quercetin, myricetin, rosmarinic acid, hesperidin, diosmetin and withanolide G) fulfilled the criteria provided by combined parameters of Lipinski's Ro5, ADMET and drug-likeness properties than reference drug nafamostat.

MD simulation analysis was carried out to find out the stability of complexes, which are formed during the docking study of the best hit of PDNPs against each of the SARS-CoV-2 variants studied here. Our observations showed no sudden surge in RMSD plots during the whole simulation time, suggesting that all complexes are stable. Moreover, fluctuations in RMSF were in the permissible range that maintained the integrity of protein-ligand interactions. Results of Rg values revealed that rutin, hesperidin, EGCG and rosmarinic acid do not induce conformational changes and showed similar compactness in protein structure during the entire MD simulation in our study. During SASA analysis, the binding of all nine PDNPs with the S-glycoproteins of all variants induce very little conformational changes, which means that the interacting sites are well exposed and readily accessible to the solvents. In order to determine the molecular interactions, a number of hydrogen bonds and hydrophobic bonds as well as water bridges were observed in all the complexes obtained through simulation, which again explained the conformational stability.

In our findings, the chemical reactivity of the best hits was obtained through geometry optimization along with the calculation of the HOMO-LUMO energy gap and MEP method on the DFT/B3LYP method at 6-311G basis set. After performing the DFT analysis, we found that rutin, hesperidin, EGCG and rosmarinic acid were more reactive than nafamostat, a reference drug. The highly chemically reactive MEP map has a great impact on a higher biological efficacy of drug leads as inhibitors and in this case, our best hits passed these barriers and thus, must be developed as inhibitors of S-glycoproteins of SARS-CoV-2 variants. Based on the computed results, it was quite significant that rutin, hesperidin, EGCG and rosmarinic acid, among the selected ones, are the best hits to have potential

binding affinities, which were better than reference drug “nafamostat” binding affinities against aforementioned variants of SARS-CoV-2. Along with previous reports on antiviral activities, the present study has given us the warrant to justify that rutin, hesperidin, EGCG and rosmarinic acid may serve as promising leads for further optimization and drug development processes to manage the COVID-19 infection via inhibiting SARS-CoV-2 virus and its variants. We suggest here that adequate preclinical and clinical study and their validations are urgently needed to establish the therapeutic efficacy of these compounds either alone or in combination for the management of COVID-19 infection.

5. Conclusions

In conclusion, a total of 100 plant-derived natural products were subjected to molecular docking, molecular dynamic (MD) simulation and DFT studies in order to identify the small molecule inhibitors against S-glycoprotein of SARS-CoV-2 variants. All the PDNPs that were tested were found to exhibit a strong affinity for the catalytic pockets of certain residues. Hesperidin, withanolide G and rosmarinic acid were identified as the three best inhibitory agents against the alpha variant; EGCG, diosmetin and myricetin were against the beta variant; rosmarinic acid, epicatechin and quercetin were against the gamma variant; rutin, EGCG and hesperidin were against the delta variant; and hesperidin against the omicron variant. Thus, based on the results of our in silico investigation, it is clear that rutin, EGCG, hesperidin, withanolide G, rosmarinic acid, diosmetin, myricetin, epicatechin and quercetin could serve as potential inhibitors against the S-glycoprotein of SARS-CoV-2 novel variants. Further in vitro and in vivo research to more clearly establish their efficacy as potential COVID-19 therapeutics is currently underway in our laboratory.

Supplementary Materials: The following supporting information can be downloaded at: <https://www.mdpi.com/article/10.3390/futurepharmacol2040034/s1>, Table S1: Docking scores of plant-derived natural products (PDNPs) against omicron (PDB ID: 7QO7); Table S2: Docking scores of plant-derived natural products (PDNPs) against delta (PDB ID: 7W92); Table S3: Docking scores of plant-derived natural products (PDNPs) against alpha (PDB ID: 8DLI); Table S4: Docking scores of plant-derived natural products (PDNPs) against beta (PDB ID: 7LYQ); Table S5: Docking scores of plant-derived natural products (PDNPs) against gamma (PDB ID: 7SBT).

Author Contributions: Conceptualization, M.F.K.; Data curation, W.A.A., M.A.K. and K.A.; Formal analysis, W.A.A. and F.R.; Supervision, M.F.K.; Writing—original draft, M.F.K.; Writing—review & editing, M.K.H. and M.S. All authors have read and agreed to the published version of the manuscript.

Funding: This research work has been financially supported by intramural funding at Era’s Lucknow Medical College, Era University, Lucknow-226003, India.

Institutional Review Board Statement: Not applicable.

Informed Consent Statement: Not applicable.

Data Availability Statement: All the docking and other computational data related to this research work have been generated in our institute with the help of the requisite systems and has been reported accordingly in the manuscript.

Acknowledgments: Authors are very thankful to the management team of Era University, Lucknow, India, and American University of Barbados (AUB) for their assistance during this work.

Conflicts of Interest: The authors declare no conflict of interest.

References

1. Zhu, Z.; Lian, X.; Su, X.; Wu, W.; Marraro, G.A.; Zeng, Y. From SARS and MERS to COVID-19: A Brief Summary and Comparison of Severe Acute Respiratory Infections Caused by Three Highly Pathogenic Human Coronaviruses. *Respir. Res.* **2020**, *21*, 224. [[CrossRef](#)] [[PubMed](#)]
2. Naqvi, A.A.T.; Fatima, K.; Mohammad, T.; Fatima, U.; Singh, I.K.; Singh, A.; Atif, S.M.; Hariprasad, G.; Hasan, G.M.; Hassan, M.I. Insights into SARS-CoV-2 Genome, Structure, Evolution, Pathogenesis and Therapies: Structural Genomics Approach. *Biochim. Biophys. Acta (BBA)-Mol. Basis Dis.* **2020**, *1866*, 165878. [[CrossRef](#)] [[PubMed](#)]

3. Ahamad, S.; Branch, S.; Harrelson, S.; Hussain, K.; Saquib, M.; Khan, S. Primed for global coronavirus pandemic: Emerging research and clinical outcome. *Eur. J. Med. Chem.* **2021**, *209*, 112862. [[CrossRef](#)] [[PubMed](#)]
4. Yang, J.; Petitjean, S.J.L.; Koehler, M.; Zhang, Q.; Dumitru, A.C.; Chen, W.; Derclaye, S.; Vincent, S.P.; Soumillion, P.; Alsteens, D. Molecular Interaction and Inhibition of SARS-CoV-2 Binding to the ACE2 Receptor. *Nat. Commun.* **2020**, *11*, 4541. [[CrossRef](#)] [[PubMed](#)]
5. Hakmaoui, A.; Khan, F.; Liacini, A.; Kaur, A.; Berka, Y.; Machraoui, S.; Soualhine, H.; Berka, N.; Rais, H.; Admou, B. Relevant SARS-CoV-2 Genome Variation through Six Months of Worldwide Monitoring. *BioMed Res. Int.* **2021**, *2021*, 5553173. [[CrossRef](#)]
6. Karunamoorthi, K.; Jegajeevanram, K.; Vijayalakshmi, J.; Mengistie, E. Traditional Medicinal Plants: A Source of Phytotherapeutic Modality in Resource-Constrained Health Care Settings. *J. Evid. Based Complement. Altern. Med.* **2013**, *18*, 67–74. [[CrossRef](#)]
7. Siddiqui, A.; Iram, F. Role of Natural Products in Drug Discovery Process. *Int. J. Drug Dev. Res.* **2014**, *6*, 172–204.
8. Levy, E.; Delvin, E.; Marcil, V.; Spahis, S. Can Phytotherapy with Polyphenols Serve as a Powerful Approach for the Prevention and Therapy Tool of Novel Coronavirus Disease 2019 (COVID-19)? *Am. J. Physiol. Endocrinol. Metab.* **2020**, *319*, E689–E708. [[CrossRef](#)]
9. Khan, M.F.; Khan, M.A.; Khan, Z.A.; Ahamad, T.; Ansari, W.A. In-Silico Study to Identify Dietary Molecules as Potential SARS-CoV-2 Agents. *Lett. Drug Des. Discov.* **2020**, *18*, 562–573. [[CrossRef](#)]
10. Ansari, W.A.; Ahamad, T.; Khan, M.A.; Khan, Z.A.; Khan, M.F. Exploration of Luteolin as Potential Anti-COVID-19 Agent: Molecular Docking, Molecular Dynamic Simulation, ADMET and DFT Analysis. *Lett. Drug Des. Discov.* **2021**, *19*, 741–756. [[CrossRef](#)]
11. Agrawal, P.K.; Agrawal, C.; Blunden, G. Rutin: A Potential Antiviral for Repurposing as a SARS-CoV-2 Main Protease (M pro) Inhibitor. *Nat. Prod. Commun.* **2021**, *16*, 1934578X21991723. [[CrossRef](#)]
12. Borse, S.; Joshi, M.; Saggam, A.; Bhat, V.; Walia, S.; Marathe, A.; Sagar, S.; Chavan-Gautam, P.; Girme, A.; Hingorani, L.; et al. Ayurveda Botanicals in COVID-19 Management: An in Silico Multi-Target Approach. *PLoS ONE* **2021**, *16*, e0248479. [[CrossRef](#)]
13. Khan, J.; Sakib, S.A.; Mahmud, S.; Khan, Z.; Islam, M.N.; Sakib, M.A.; bin Emran, T.; Simal-Gandara, J. Identification of Potential Phytochemicals from Citrus Limon against Main Protease of SARS-CoV-2: Molecular Docking, Molecular Dynamic Simulations and Quantum Computations. *J. Biomol. Struct. Dyn.* **2021**, 1–12. [[CrossRef](#)]
14. Pokharkar, O.; Lakshmanan, H.; Zyryanov, G.; Tsurkan, M. In Silico Evaluation of Antifungal Compounds from Marine Sponges against COVID-19-Associated Mucormycosis. *Mar. Drugs* **2022**, *20*, 215. [[CrossRef](#)] [[PubMed](#)]
15. Basha, S.; Tripathi, D.; Koora, S.; Satyanarayana, K.; Jayaraman, S. Molecular docking analysis of potential compounds from an Indian medicinal soup “kabsura kudineer” extract with IL-6. *Biomed. Inf.* **2021**, *17*, 568–572.
16. Sharma, V.; Sharma, P.C.; Kumar, V. In silico molecular docking analysis of natural pyridoacridines as anticancer agents. *Adv. Chem.* **2016**, 1–9. [[CrossRef](#)]
17. Goodford, P. A computational procedure for determining energetically favorable binding sites on biologically important macromolecules. *J. Med. Chem.* **1984**, *27*, 557. [[CrossRef](#)] [[PubMed](#)]
18. Ansari, W.; Rizvi, F.; Khan, M.; Khan, Z.; Khan, M. Computational Study Reveals the Inhibitory Effects of Chemical Constituents from *Azadirachta indica* (Indian Neem) Against Delta and Omicron Variants of SARS-CoV-2. *Coronaviruses* **2022**, *3*, e270822208065.
19. Sheikh, S.; Hassan, F.; Khan, M.; Ahamad, T.; Ansari, W.; Akhter, Y.; Khafagy, E.; Khan, A.; Nasibullah, M. Drug Repurposing to Discover Novel Anti-Inflammatory Agents Inhibiting JAK3/STAT Signaling. *Russ. J. Bioorg. Chem.* **2022**, *48*, 958–975. [[CrossRef](#)]
20. Khan, M.; Ansari, W.; Ahamad, T.; Khan, M.; Khan, Z.; Sarfraz, A.; Khan, M. Bioactive components of different nasal spray solutions may defeat SARS-CoV-2: Repurposing and in silico studies. *J. Mol. Model.* **2022**, *28*, 212. [[CrossRef](#)] [[PubMed](#)]
21. Saini, M.; Sangwan, R.; Khan, M.; Kumar, A.; Verma, R.; Jain, S. Specioside (SS) & verminoside (VS) (Iridoid glycosides): Isolation, characterization and comparable quantum chemical studies using density functional theory (DFT). *Heliyon* **2019**, *5*, e1118.
22. Thangavel, N.; Al Bratty, M.; Al Hazmi, H.; Najmi, A.; Alaqi, R. Molecular Docking, and Molecular Dynamics Aided Virtual Search of OliveNet™ Directory for Secoiridoids to Combat SARS-CoV-2 Infection and Associated Hyperinflammatory Responses. *Front. Mol. Biosci.* **2021**, *7*, 627767. [[CrossRef](#)] [[PubMed](#)]
23. Srivastava, V.; Yadav, A.; Sarkar, P. Molecular docking and ADMET study of bioactive compounds of *Glycyrrhiza glabra* against main protease of SARS-CoV-2. *Mater. Today Proc.* **2022**, *49*, 2999–3007. [[CrossRef](#)] [[PubMed](#)]
24. Lin, X.; Li, X.; Lin, X. A Review on Applications of Computational Methods in Drug Screening and Design. *Molecules* **2020**, *25*, 1375. [[CrossRef](#)]
25. Gurung, A.; Ali, M.; Elshikh, M.; Aref, I.; Amina, M.; Lee, J. An in silico approach unveils the potential of antiviral compounds in preclinical and clinical trials as SARS-CoV-2 omicron inhibitors. *Saudi J. Biol. Sci.* **2022**, *29*, 103297. [[CrossRef](#)]
26. Muhammad, S.; Fatima, N. In Silico Analysis and Molecular Docking Studies of Potential Angiotensin-Converting Enzyme Inhibitor Using Quercetin Glycosides. *Pharmacogn. Mag.* **2015**, *11*, 123. [[CrossRef](#)]
27. Jayaraman, A.; Jamil, K. Drug Targets for Cell Cycle Dysregulators in Leukemogenesis: In Silico Docking Studies. *PLoS ONE* **2014**, *9*, e86310. [[CrossRef](#)] [[PubMed](#)]
28. Sixto-López, Y.; Correa-Basurto, J.; Bello, M.; Landeros-Rivera, B.; Garzón-Tiznado, J.A.; Montaña, S. Structural Insights into SARS-CoV-2 Spike Protein and Its Natural Mutants Found in Mexican Population. *Sci. Rep.* **2021**, *11*, 4659. [[CrossRef](#)] [[PubMed](#)]
29. Al-Karmalawy, A.A.; Dahab, M.A.; Metwaly, A.M.; Elhady, S.S.; Elkaeed, E.B.; Eissa, I.H.; Darwish, K.M. Molecular Docking and Dynamics Simulation Revealed the Potential Inhibitory Activity of ACEIs Against SARS-CoV-2 Targeting the HACE2 Receptor. *Front. Chem.* **2021**, *9*, 661230. [[CrossRef](#)] [[PubMed](#)]

30. Mahmoud, A.; Mostafa, A.; Al-Karmalawy, A.A.; Zidan, A.; Abulkhair, H.S.; Mahmoud, S.H.; Shehata, M.; Elhefnawi, M.M.; Ali, M.A. Telaprevir Is a Potential Drug for Repurposing against SARS-CoV-2: Computational and in Vitro Studies. *Heliyon* **2021**, *7*, e07962. [[CrossRef](#)] [[PubMed](#)]
31. Bhowmick, S.; Saha, A.; Osman, S.M.; Alasmary, F.A.; Almutairi, T.M.; Islam, M.A. Structure-Based Identification of SARS-CoV-2 Main Protease Inhibitors from Anti-Viral Specific Chemical Libraries: An Exhaustive Computational Screening Approach. *Mol. Divers.* **2021**, *25*, 1979–1997. [[CrossRef](#)]
32. Dhankhar, P.; Dalal, V.; Kotra, D.; Kumar, P. In-silico approach to identify novel potent inhibitors against GraR of *S. aureus*. *Front. Biosci.* **2020**, *25*, 1337–1360.
33. Hassan, M.; Shahzadi, S.; Seo, S.Y.; Alashwal, H.; Zaki, N.; Moustafa, A.A. Molecular Docking and Dynamic Simulation of AZD3293 and Solanezumab Effects against BACE1 to Treat Alzheimer's Disease. *Front. Comput. Neurosci.* **2018**, *12*, 34. [[CrossRef](#)]
34. Verma, S.; Grover, S.; Tyagi, C.; Goyal, S.; Jamal, S.; Singh, A.; Grover, A. Hydrophobic Interactions Are a Key to MDM2 Inhibition by Polyphenols as Revealed by Molecular Dynamics Simulations and MM/PBSA Free Energy Calculations. *PLoS ONE* **2016**, *11*, e0149014. [[CrossRef](#)]
35. Abdalla, M.; Mohapatra, R.K.; Sarangi, A.K.; Mohapatra, P.K.; Eltayb, W.A.; Alam, M.; El-Arabey, A.A.; Azam, M.; Al-Resayes, S.I.; Seidel, V.; et al. In Silico Studies on Phytochemicals to Combat the Emerging COVID-19 Infection. *J. Saudi Chem. Soc.* **2021**, *25*, 101367. [[CrossRef](#)]
36. Waqas Alam, M.; Farhan, M.; Souayah, B.; Aamir, M.; Khan, M.S. Synthesis, Crystal Structure, Density Functional Theory (DFT) Calculations and Molecular Orbital Calculations of 4-Bromoanilinium Perchlorate Single Crystal. *Crystals* **2021**, *11*, 1070. [[CrossRef](#)]
37. Arivazhagan, M.; Kumar, J. Molecular structure, vibrational spectral assignments, HOMO–LUMO, MESP, Mulliken analysis and thermodynamic properties of 2,6-xylenol and 2,5-dimethyl cyclohexanol based on DFT calculation. *Spectrochim. Acta A* **2015**, *137*, 490–502. [[CrossRef](#)] [[PubMed](#)]
38. Sanches, P.R.S.; Charlie-Silva, I.; Braz, H.L.B.; Bittar, C.; Freitas Calmon, M.; Rahal, P.; Cilli, E.M. Recent Advances in SARS-CoV-2 Spike Protein and RBD Mutations Comparison between New Variants Alpha (B.1.1.7, United Kingdom), Beta (B.1.351, South Africa), Gamma (P.1, Brazil) and Delta (B.1.617.2, India). *J. Virus Erad.* **2021**, *7*, 100054. [[CrossRef](#)] [[PubMed](#)]
39. Pascarella, S.; Ciccozzi, M.; Zella, D.; Bianchi, M.; Benedetti, F.; Benvenuto, D.; Broccolo, F.; Cauda, R.; Caruso, A.; Angeletti, S.; et al. SARS-CoV-2 B.1.617 Indian Variants: Are Electrostatic Potential Changes Responsible for a Higher Transmission Rate? *J. Med. Virol.* **2021**, *93*, 6551–6556. [[CrossRef](#)]
40. Adhikari, B.; Marasini, B.; Rayamajhee, B.; Bhattarai, B.; Lamichhane, G.; Khadayat, K.; Adhikari, A.; Khanal, S.; Parajuli, N. Potential roles of medicinal plants for the treatment of viral diseases focusing on COVID-19: A review. *Phytother. Res.* **2021**, *35*, 1298–1312. [[CrossRef](#)] [[PubMed](#)]
41. Santana, F.P.R.; Pinheiro, N.M.; Mernak, M.I.B.; Righetti, R.F.; Martins, M.A.; Lago, J.H.G.; Lopes, F.D.T.Q.D.S.; Tibério, I.F.L.C.; Prado, C.M. Evidences of Herbal Medicine-Derived Natural Products Effects in Inflammatory Lung Diseases. *Mediat. Inflamm.* **2016**, *2016*, 2348968. [[CrossRef](#)] [[PubMed](#)]
42. Montenegro-Landívar, M.; Tapia-Quirós, P.; Vecino, X.; Reig, M.; Valderrama, C.; Grandos, M.; Luis Cortina, J.; Saurina, J. Polyphenols and their potential role to fight viral diseases: An overview. *Sci. Total Environ.* **2021**, *801*, 149719. [[CrossRef](#)] [[PubMed](#)]
43. Chojnacka, K.; Skrzypczak, D.; Izydorczyk, G.; Mikula, K.; Szopa, D.; Witek-Krowiak, A. Antiviral Properties of Polyphenols from Plants. *Foods* **2021**, *10*, 2277. [[CrossRef](#)]
44. Chen, Y.; Kirchmair, J. Cheminformatics in Natural Product-based Drug Discovery. *Mol. Inform.* **2022**, *39*, 2000171. [[CrossRef](#)] [[PubMed](#)]
45. Muratov, E.; Amaro, R.; Andrade, C.; Brown, N.; Ekins, S.; Fourches, D.; Isayev, O.; Kozakov, D.; Medina-Franco, J.; Merz, K.; et al. A critical overview of computational approaches employed for COVID-19 drug discovery. *Chem. Soc. Rev.* **2021**, *50*, 9121. [[CrossRef](#)] [[PubMed](#)]
46. Macip, G.; Garcia-Segura, P.; Mestres-Truyol, J.; Saldivar-Espinoza, B.; Ojeda-Montes, M.; Gimeno, A.; Cereto-Massgué, A.; Garcia-Vallvé, S.; Pujadas, G. Haste make waste: A critical review of docking –based virtual screening in drug repurposing for SARS-CoV-2 main protease (Mpro) inhibition. *Med. Res. Rev.* **2021**, *42*, 744–769. [[CrossRef](#)] [[PubMed](#)]
47. Liu, J.; Bodnar, B.H.; Meng, F.; Khan, A.I.; Wang, X.; Saribas, S.; Wang, T.; Lohani, S.C.; Wang, P.; Wei, Z.; et al. Epigallocatechin gallate from green tea effectively blocks infection of SARS-CoV-2 and new variants by inhibiting spike binding to ACE2 receptor. *Cell Biosci.* **2021**, *11*, 168. [[CrossRef](#)]
48. Haggag, Y.A.; El-Ashrawy, N.E.; Okasha, K.M. Is Hesperidin Essential for Prophylaxis and Treatment of COVID-19 Infection? *Med. Hypotheses* **2020**, *144*, 109957. [[CrossRef](#)]
49. Cheng, F.; Huynh, T.; Yang, C.; Hu, D.; Shen, Y.; Tu, C.; Wu, Y.; Tang, C.; Huang, W.; Chen, Y.; et al. Hesperidin Is a Potential Inhibitor against SARS-CoV-2 Infection. *Nutrients* **2021**, *13*, 2800. [[CrossRef](#)]
50. Ferreira, J.; Fadl, S.; Villanueva, A.; Rabeh, W. Catalytic Dyad Residues His41 and Cys145 Impact the Catalytic Activity and Overall Conformational Fold of the Main SARS-CoV-2 Protease 3-Chymotrypsin-Like Protease. *Front. Chem.* **2021**, *9*, 692168. [[CrossRef](#)]

51. Xiao, T.; Cui, M.; Zheng, C.; Wang, M.; Sun, R.; Gao, D.; Bao, J.; Ren, S.; Yang, B.; Lin, J.; et al. Myricetin Inhibits SARS-CoV-2 Viral Replication by Targeting Mpro and Ameliorates Pulmonary Inflammation. *Front. Pharmacol.* **2021**, *12*, 669642. [[CrossRef](#)] [[PubMed](#)]
52. Tripathi, M.K.; Singh, P.; Sharma, S.; Singh, T.P.; Ethayathulla, A.S.; Kaur, P. Identification of Bioactive Molecule from *Withania Somnifera* (Ashwagandha) as SARS-CoV-2 Main Protease Inhibitor. *J. Biomol. Struct. Dyn.* **2020**, *39*, 5668–5681. [[CrossRef](#)] [[PubMed](#)]
53. Straughn, A.R.; Kakar, S.S. Withaferin A: A Potential Therapeutic Agent against COVID-19 Infection. *J. Ovarian Res.* **2020**, *14*, 126. [[CrossRef](#)]
54. Elebeedy, D.; Elkhatib, W.F.; Kandeil, A.; Ghanem, A.; Kutkat, O.; Alnajjar, R.; Saleh, M.A.; Abd El Maksoud, A.I.; Badawy, I.; Al-Karmalawy, A.A. Anti-SARS-CoV-2 Activities of Tanshinone IIA, Carnosic Acid, Rosmarinic Acid, Salvianolic Acid, Baicalein, and Glycyrrhetic Acid between Computational Andin Vitroinsights. *RSC Adv.* **2021**, *11*, 29267–29286. [[CrossRef](#)]
55. Oselusi, S.O.; Christoffels, A.; Egieyeh, S.A. Cheminformatic Characterization of Natural Antimicrobial Products for the Development of New Lead Compounds. *Molecules* **2021**, *26*, 3970. [[CrossRef](#)]
56. Guan, L.; Yang, H.; Cai, Y.; Sun, L.; Di, P.; Li, W.; Liu, G.; Tang, Y. ADMET-Score-a Comprehensive Scoring Function for Evaluation of Chemical Drug-Likeness. *Med. Chem. Commun.* **2019**, *10*, 148–157. [[CrossRef](#)] [[PubMed](#)]